Chapter 6

Optimization of Diesel Engine with Dual-Loop EGR by Using DOE Method

Jungsoo Park and Kyo Seung Lee

Additional information is available at the end of the chapter

http://dx.doi.org/10.5772/55861

1. Introduction

The diesel engine has advantages in terms of fuel consumption, combustion efficiency and durability. It also emits lower carbon dioxide (CO_2), carbon monoxide(CO) and hydrocarbons(HC). However, diesel engines are the major source of NOx and particulate matter emissions in urban areas. As the environmental concern increases, a reduction of NOx emission is one of the most important tasks for the automotive industry. In addition, future emission regulations require a significant reduction in both NOx and particulate matter by using EGR and aftertreatment systems (Johnson, 2011).

Exhaust gas recirculation (EGR) is an emission control technology allowing significant NOx emission reductions from light- and heavy-duty diesel engines. The key effects of EGR are lowering the flame temperature and the oxygen concentration of the working fluid in the combustion chamber (Zheng et al., 2004).

There are conventional types of EGR, high pressure loop and low pressure loop EGR. Table 1 shows advantages and drawbacks of each type of EGR.

	Advantages	Drawbacks
HPL EGR	• Lower HC and CO emissions • Fast response time	• Cooler fouling • Unstable cylinder-by-cylinder EGR distribution
LPL EGR	• High cooled EGR • Clean EGR (no fouling) • Stable cylinder-by-cylinder EGR distribution • Better Φ/EGR rate	• Corrosion of compressor wheel due to condensation water • Slow response time • HC/CO increase

Table 1. Advantages and different types of EGR

Because a HPL EGR has fast response, especially at lower speed and load, it is only applicable when the turbine upstream pressure is sufficiently higher than the boost pressure. For the LPL EGR, a positive differential pressure between the turbine outlet and the compressor inlet is generally needed. However, LPL EGR has slow response than that of HPL systems, especially at low load or speed (Yamashita et al., 2011). Facing the reinforced regulations, exhaust gas recirculation system is widely used and believed to be a very effective method for NOx and PM reductions. Furthermore, increasing needs of low temperature combustion (LTC), EGR have been issued as key technology expecting to provide heavy EGR rate and newly developed dual loop EGR system as the future of EGR types has became a common issue.

The experimental results of dual loop EGR systems were reported in Cho et al. (2008) who studied high efficiency clean combustion (HECC) engine for comparison between HPL, LPL and dual loop EGR at five operating conditions. Adachi et al.(2009) and Kobayashi et al.(2011) reported that The combination of both high boost pressure by turbocharger and a high rate of EGR are effective to reduce BSNOx and PM emissions. Especially, The EGR system using both high-pressure loop EGR and low-pressure loop EGR is also effective to reduce BSNOx and PM emissions because it maintains higher boost pressure than that of the high-pressure loop EGR system alone.

It was also reported that determination of the intake air/exhaust gas fraction by proper control logic (Wang, 2008; Yan & Wang, 2010, 2011) and turbocharger matching (Shutty, 2009) was important. However, there was more complex interaction between variables affecting the total engine system. Therefore, it is necessary to identify dominant variables at specific operating conditions to understand and provide adaptive and optimum control logic.

One of the optimization methods, design of experiment (DOE), can provide the dominant variables which have effects on dependent variables at specified operating conditions. Lee et al.(2006) studied the low pressure EGR optimization by using the DOE in a heavy-duty diesel engine for EURO 5 regulation. The dominant variables that had effects on torque, NOx and EGR rate were EGR valve opening rate, start of injection and injection mass. In their study, the optimized LPL EGR system achieved 75% NOx reduction with 6% increase of BSFC.

In this study, as one of the future EGR types, the dual loop EGR system which had combining features of high pressure loop EGR and low pressure loop EGR was developed and optimized to find the dominant parameter under frequent engine operating conditions by using a commercial engine simulation code and design of experiment (DOE). Results from the simulation are validated with experimental results.

2. Engine model

2.1. Engine specification

The engine specification used to model is summarized in Table 2. An original engine was equipped with a variable geometry turbocharger (VGT), intercooler and HPL EGR system.

Operating parameters included engine operating speed, fuel flow rate, ambient conditions, and combustion data. In addition, the length of connecting rods, distance between the piston and pin, compression ratio, and the coefficient of friction were collected and entered in GT-POWER. Data sets of valve diameters, valve timing, injection timing, duration and injection pressure were also acquired. These data were classified information of the engine manufacturer and could not be listed in detail. Engine operating conditions are summarized in Table 3.

Item	Specification
Engine volume	3 liter
Cylinder arrangement	6cyl., V- type
Bore, Stroke	84, 89mm
Compression ratio	17.3
Connecting rod length	159 mm
Wrist pin to crank offset	0.5mm
Firing order	1-3-4-2-5-6
Firing intervals	120 CA
Injection type EGR system	Common rail High pressure EGR system
Max. torque@rpm	240PS@3800rpm
Max. power@rpm	450N-m@1720~3500rpm

Table 2. Engine specifications

Case #	RPM	BMEP (bar)
1	732	2.17
2	1636	4.66
3	1422	3.66
4	1556	9.93
5	1909	8.80

Table 3. Engine operating conditions

The selected 5 operating conditions in the analysis were picked up from frequently operated region at emission test point given by engine manufacturer.

2.2. Engine analysis tool

Simulations were carried out by using commercial 1D code, GT-POWER, which is designed for steady-state and transient simulations and can be used for analyses of engine and powertrain control. It is based on one-dimensional gas dynamics, representing the flow and heat transfer in the piping and in the other components of an engine system. The complicated shape of intake and exhaust manifolds were converted from 3D models (by using CATIA originally) to 1D models by 3D-discretizer. Throughout the conversion, analysis of gas flow and dynamics could be faster and easier under 1D flow environment.

The combustion model was the direct-injection diesel jet (DI jet) model and it was primarily used to predict the burn rate and NOx emission simultaneously.

2.2.1. Overview of DI jet

The combustion model, DI jet, was firstly introduced by Hiroyasu known as a multi-zone DI diesel spray combustion (Hiroyasu et al., 1983). The core approach of this model is to track the fuel jet as it breaks into droplets, evaporates, mixes and burns. As such an accurate injection profile is absolutely required to achieve meaningful results. The total injected fuel is broken up into packages (also referred as zones): 5 radial and many axial slices. Each package additionally contains parcels (or subzones) for liquid fuel, unburned vapor fuel and entrained air, and burned gases.

The total mass of fuel in all of the packages will be equal to the specified injection rate (mg/stroke) divided by the specified number of nozzle holes, as DI jet will model the plume from only one nozzle hole.

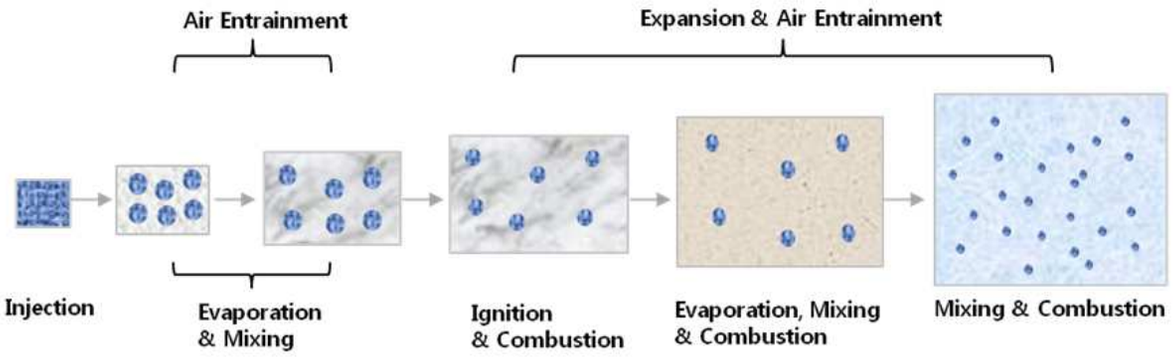

Figure 1. Air-fuel mixing process within each package

The occurring processes in the package are shown in Figure 1. The package, immediately after the fuel injection, involves many fine droplets and a small volume of air. As the package recedes from the nozzle, the air entrains into the package and fuel droplets evaporate. Therefore, the small package consists of liquids fuel, vaporized fuel and air. After a short period of time from the injection, ignition occurs in the gaseous mixture resulting in sudden expansion of the package. Thereafter, the fuel droplets evaporate, and fresh air entrains into the package. Vaporized fuel mixes with fresh air and combustion products and spray continues to burn.

2.2.2. Combustion process of DI jet

Figure 2 shows the detailed combustion process of each package in DI jet model (Hiroyasu et al, 1983). When ignition is occurred, the combustible mixture which is prepared before ignition burns in small increment of time. Combustion rate and amount of burning fuel of each package are calculated by assuming the stoichiometric condition. When the air in the package is enough for burning the vaporized fuel, there are combustion products, liquid

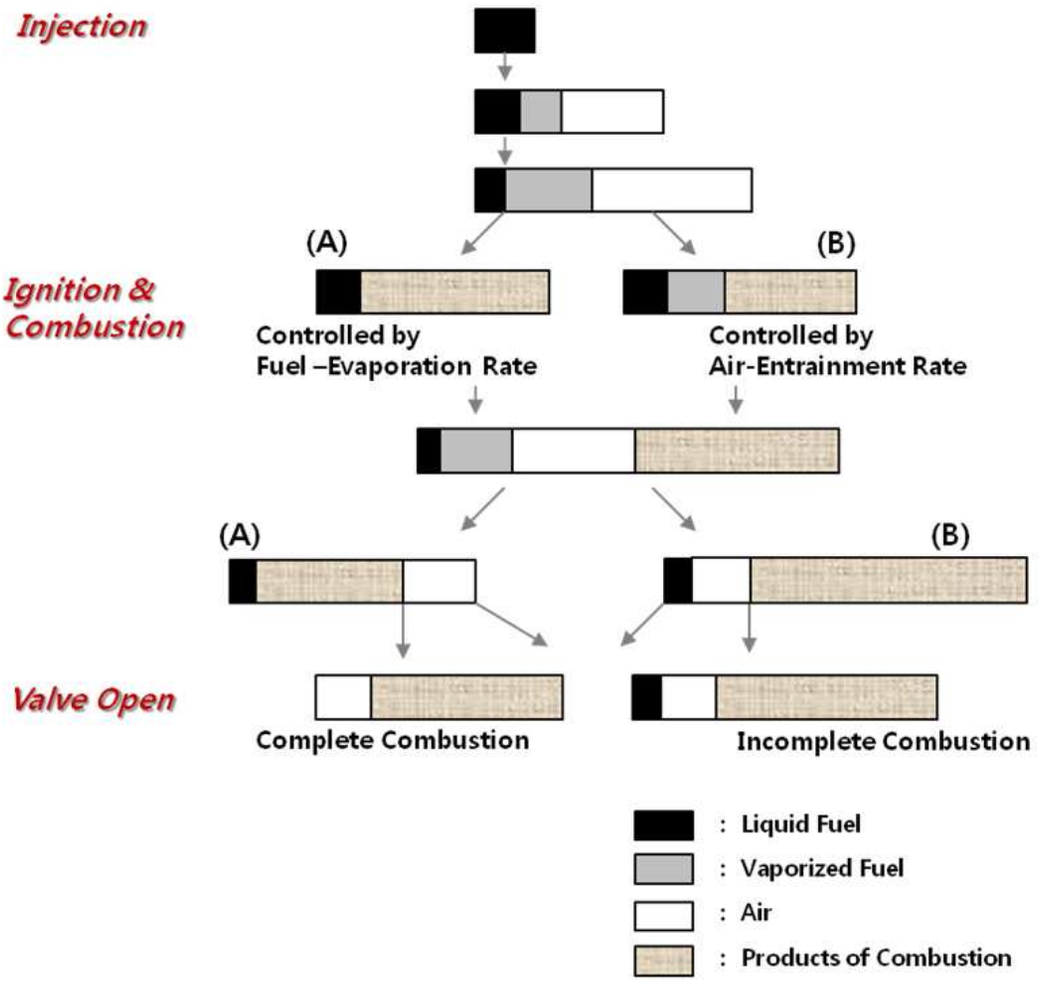

Figure 2. Schematic diagram of the mass system in a package

fuel and the remained air in the package after ignition occurs. In the next small increment of time, the fuel droplets evaporate and fresh air entrains in the package. The combustion of the next step occurs (case A in figure 2). After this step, since the stoiciometric combustion is assumed, either the vaporized fuel or the air is remained. When the air is remained, the same combustion process is repeated. But when the vaporized fuel is remained, the amount of burning fuel is controlled by the entrained air in the next step (case B in Figure 2). If ignition occurs, but the air in the package is not enough for burning the vaporized fuel, the combustion process continues under the condition shown in case B. Therefore, all the combustion processes in each package proceed under one of the conditions shown in Figure 2; Case A is evaporation rate control combustion, and B is entrainment rate control combustion. The heat release rate in the combustion chamber is calculated by summing up the heat release of each package. The pressure and average temperature in the cyinder are then calculated. Since the time histories of temperature, vaporized fuel, air and combustion products in each package are known, the equilibrium concentrations of gas compositions in the package can be calculated. The concentration of NOx is calculated by using the extended Zeldovich mechanism. More detailed governing equations can be found in Hiroyasu's studies (Hiroyasu et al, 1983).

2.3. Engine model with HPL EGR

Based on experimental data, an engine model with HPL EGR was designed. Boost pressure was matched at appropriate turbocharger speeds based on turbine and compressor maps. The injection duration at a given injection timing, injection pressure, combustion pressure and temperature were determined. Then, back pressure at the turbine downstream and EGR valve opening were determined. EGR rate, temperature and pressure drop after the EGR cooler was monitored by installing actuators and sensors. Finally, results of the simulation were compared to the experimental data. Figure 3 shows the Engine model with HPL EGR.

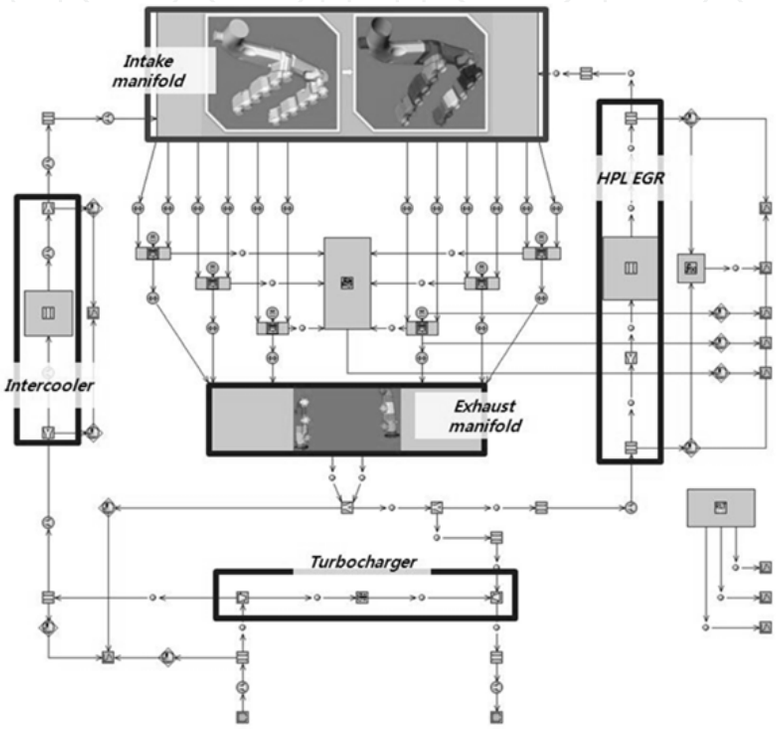

Figure 3. Engine model with HPL EGR

The percent of exhaust gas recirculation (EGR (%)) is defined as following equation.

$$EGR(\%) = \left(m_{EGR} / m_i\right) \times 100 \quad (1)$$

where [$m_i = m_a + m_f + m_{EGR}$] and m_{EGR} is the mass of EGR and m_a and m_f are the mass of air and fuel.

2.4. Engine model with dual loop EGR system and optimization

Based on the HPL model, a dual loop EGR model was designed. Comparing to the HPL EGR system, flap valve opening rate became one of the most important variables for pressure difference at P_2-P_1 in Figure 4.

First, Dual loop EGR simulation was performed under constant boost pressure. Flap valve opening at tail pipe and turbocharger RPM, which had effects on boost pressure and back

pressure under dual loop EGR system, were selected as independent variables. In this case, NOx reduction rate would increase, but torque and BSFC would decrease. And the next step, optimization was performed to compensate torque loss and brake specific fuel consumption (BSFC) by modifying injection mass, start of injection (SOI) and EGR valve opening rate. Results of simulation were compared to the HPL and dual loop models in terms of torque, EGR rate, BSNOx, and BSFC.

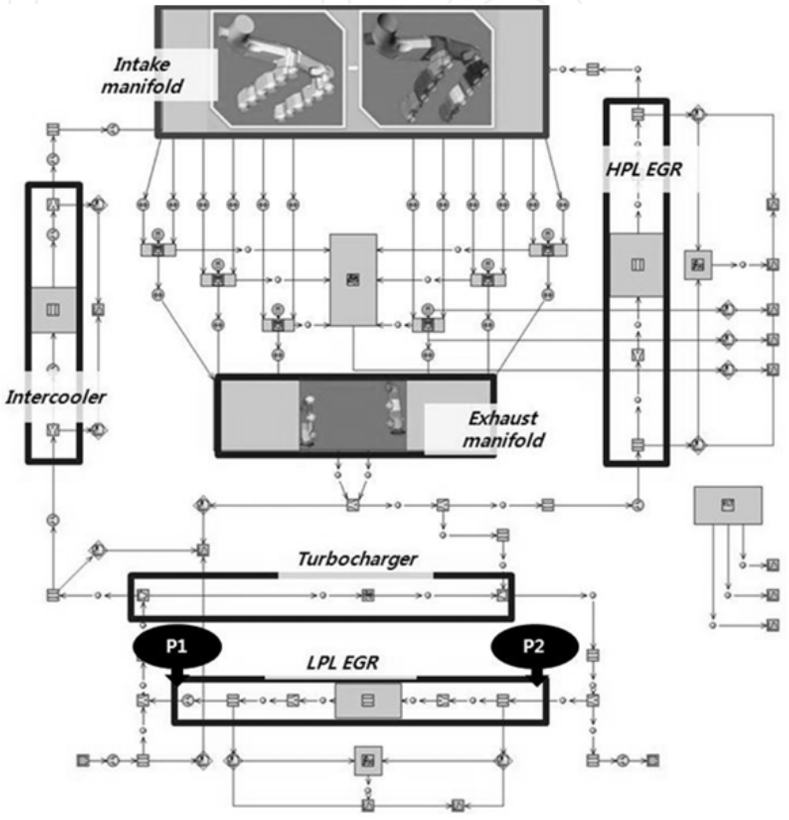

Figure 4. Engine model with dual-loop EGR

2.5. Design of experiment (DOE)

In this study, optimization based on DOE was performed.

There are main variables which have major effects on torque, BSNOx, BSFC, and EGR rate. In this study, 6 independent variables were selected such as HPL EGR valve opening diameter, LPL EGR valve opening diameter, injection mass, start of injection (SOI), flap valve opening diameter at the tail pipe and turbocharger RPM (TC RPM). Then proper ranges were set and DOE was performed based on the full factorial design.

Torque, EGR rate, BSNOx, BSFC and boost pressure were selected as response variables. The range of each independent variable was chosen based on the engine design performance.

Table 4 shows control factors and levels for optimization of the dual EGR system.

Control factor		Level 1	Level 2	Level 3
EGR valve	HPL	base	15% open	30% open
	LPL	base	15% open	30% open
Injection mass		base	+2.5%	+5%
SOI		3 CA adv.	1.5 CA adv.	base.
Flap valve		15% close	Base	15% open
TC RPM		-5000 RPM	base	+5000 RPM
Full factorial		$3^6 = 729$		

Table 4. Control factors and levels for optimization of the dual EGR system

2.5.1. Control factors

The 6 independent variables were selected, i.e. HPL EGR valve opening diameter, LPL EGR valve opening diameter, injection mass, start of injection (SOI), flap valve opening diameter at the tail pipe and turbocharger RPM (TC RPM). And their desired ranges are as follows. Base level means the values given by the experimental test.

- HPL & LPL EGR valves: If the EGR valve opens too much, it causes torque loss. In this optimization, the maximum increase of EGR valve diameter was 30% at the given operating conditions from the values under constant boost pressure.
- Injection mass: 5% increase of injection mass was selected and increasing injection mass had an effect on BSNOx. However, it normally degraded BSFC.
- SOI: In general, injection starts faster than 25-23° CA bTDC. If fuel were injected too early, imperfect combustion could degrade the engine performance. In this optimization the maximum advanced CA selected was 3 from the current value which could be within the ranges. Advanced SOI could increase torque without any other variable changes. Also, the EGR rate could increase up to 10% .
- Flap valve and TC RPM: Under dual loop EGR system, pressure difference at P2-P1 in Figure 2 was affected by interaction between flap valve and TC RPM which had a dominant effect on EGR rate and BSNOx under the dual loop EGR system.
- Especially, TC RPM was chosen to maintain boost pressure based on the turbocharger map. Positive and negative signs mean increase and decrease of rotation speed of turbocharger shaft which is driven by the exhaust flow. This change in shaft rotation speed is to optimize and maintain target boost pressure under different exhaust energy from combustion at dual-loop EGR system.

3. Results and discussion

3.1. Validation

Table 5 shows comparisons between the experiment and the simulation data in terms of injection mass and maximum cylinder pressure. There are two pilot injections and one main injection. By separating pilot injections, combustion noise, soot and NOx can be controlled.

Total injection mass and rate of main injection were given but rate of pilot injections had to be determined by matching injection duration and pressure. Figure 5 shows the torque, EGR rate, and NOx results of the simulation and the experiment, respectively. The differences of each point were within ±5% and it was proven that the simulation results had good agreement with experimental results.

Case No.	Normalized integrated injected mass (fraction)						Maximum cylinder pressure (bar)	
	Experiment			Simulation			Experiment	Simulation
	Pilot 1	Pilot 2	Main	Pilot 1	Pilot 2	Main		
1	0.134	0.134	0.732	0.120	0.130	0.750	53	53
2	0.081	0.081	0.839	0.086	0.089	0.825	58	58
3	0.102	0.102	0.797	0.097	0.122	0.781	51	51
4	0.045	0.045	0.910	0.044	0.035	0.921	75	78
5	0.047	0.047	0.905	0.049	0.045	0.906	76	79

Table 5. Comparison between the experiment and simulation data in terms of injection mass and maximum cylinder pressure

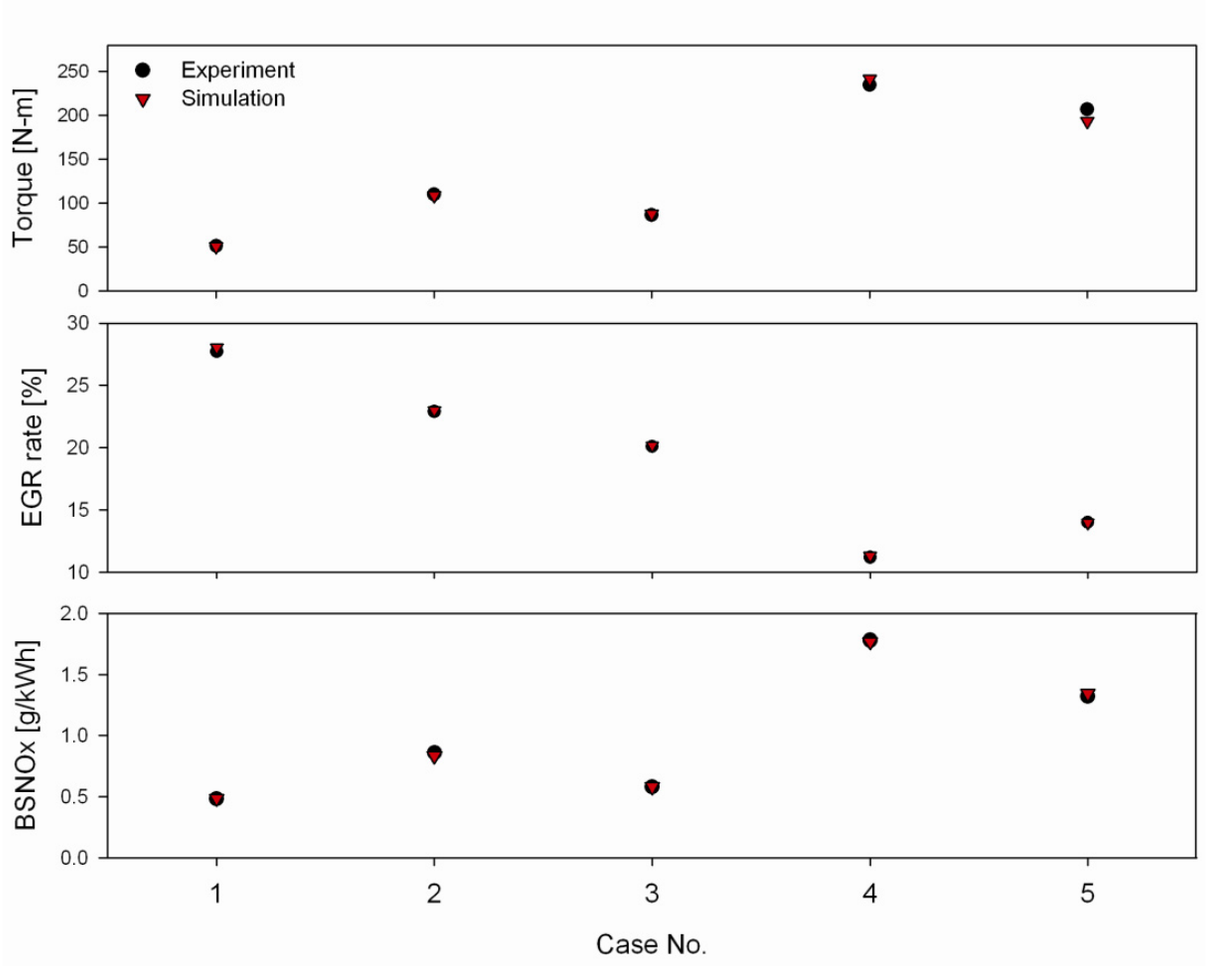

Figure 5. Comparison between experiment and simulation results: Torque, EGR rate and BSNOx

3.2. Optimization of dual-loop EGR system

Based on the DOE, response variables were determined under constant boost pressure with fixed HPL valve diameter. Then, torque and BSFC compensation were performed.

3.2.1. Optimization of dual-loop EGR system

Dual loop EGR system optimization was performed based on constant boost pressure and fixed HPL valve opening diameter to minimize torque loss. Table 6 shows the target boost pressure under dual loop EGR system which were from experiment data. Input value of HPL valve opening diameter was the same as that of the HPL model.

Case No.	1	2	3	4	5
Target boost pressure	1.03	1.23	1.11	1.43	1.56

Table 6. Target boost pressure

Figure 6 and 7 show the comparison between combustion characteristics of HPL and dual loop EGR system under constant boost pressure in case 5. Increased EGR rate caused cylinder peak pressure decrease under the dual loop EGR system. And lower peak heat release rate corresponded to lower NOx emissions.

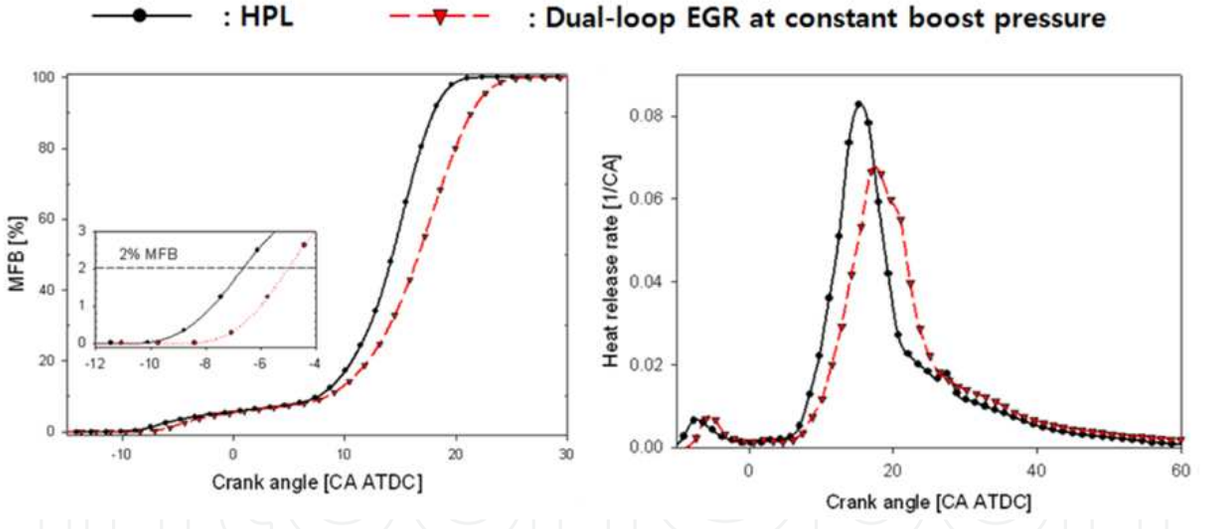

Figure 6. Mass fraction burned and heat release rate between under HPL and dual loop EGR system

Figure 8 shows the result of dual loop EGR simulation under constant boost pressure. Compared to the HPL model, 8% of torque and 8% of BSFC decreased on average. In detail, about 12 % of maximum torque loss (case 3) and about 11 % of maximum BSFC loss (case 1) occurred for the dual loop EGR. On the other hand, about 60% of NOx reduction was achieved on an average. In addition, a maximum of, 80% of NOx reduction was achieved due to the remarkable increase of the EGR rate (case 2). It seemed that the mass of the LPL EGR portion had strong effects on total NOx reduction under larger pressure difference between turbine downstream and compressor upstream. In case 3, the NOx reduction rate became lower because of smaller pressure difference at P2-P1 in Figure 4.

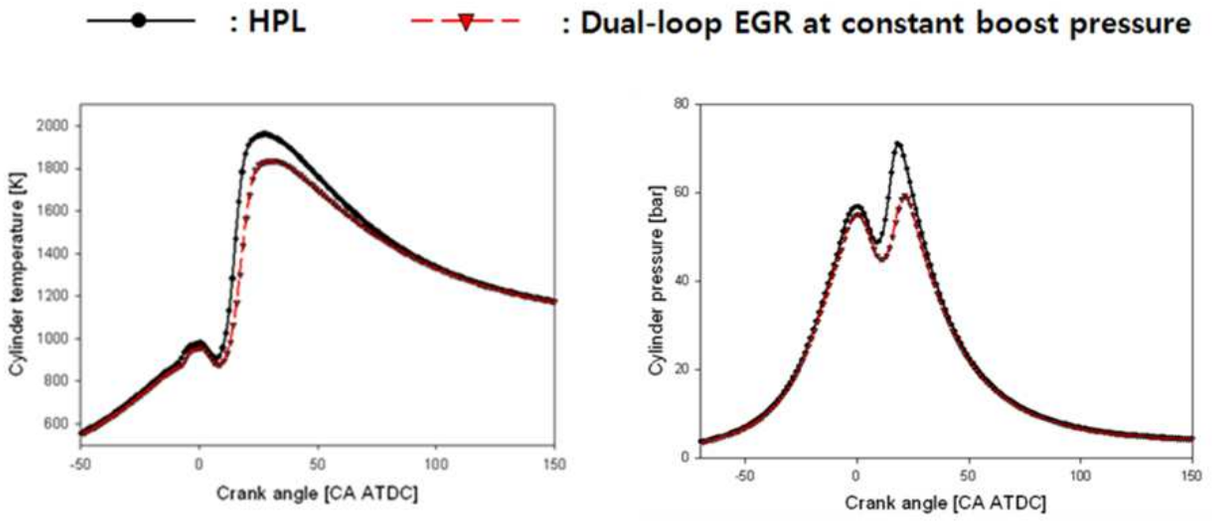

Figure 7. In-cylinder temperature and pressure trace between under HPL and dual loop EGR system

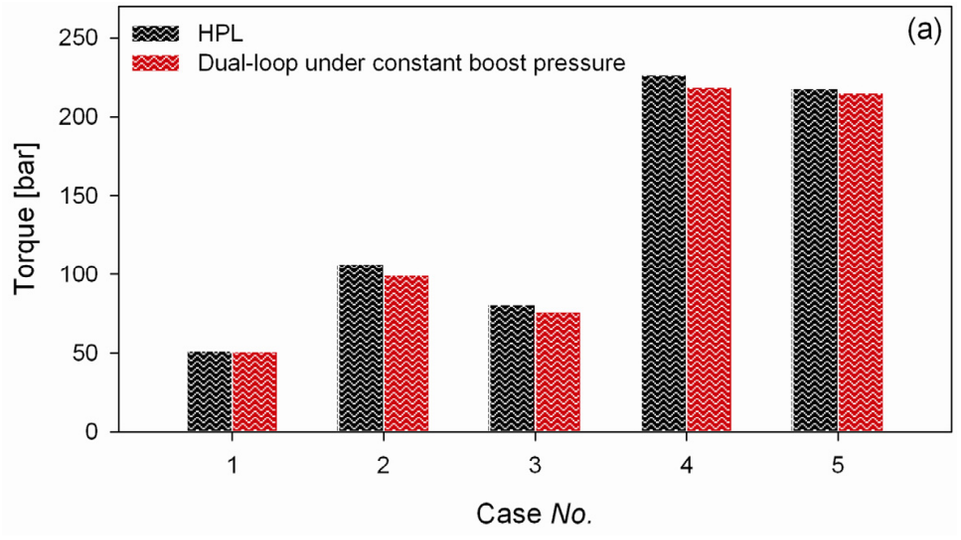

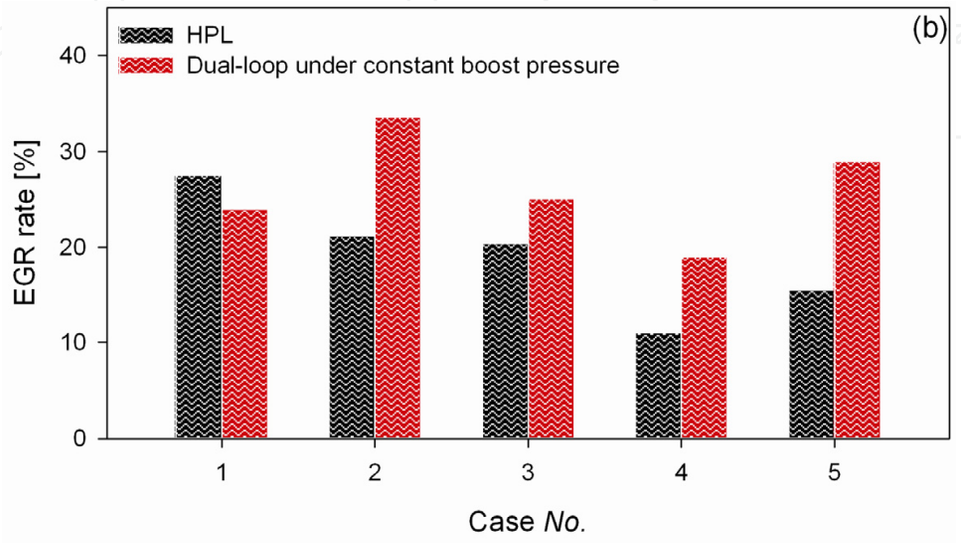

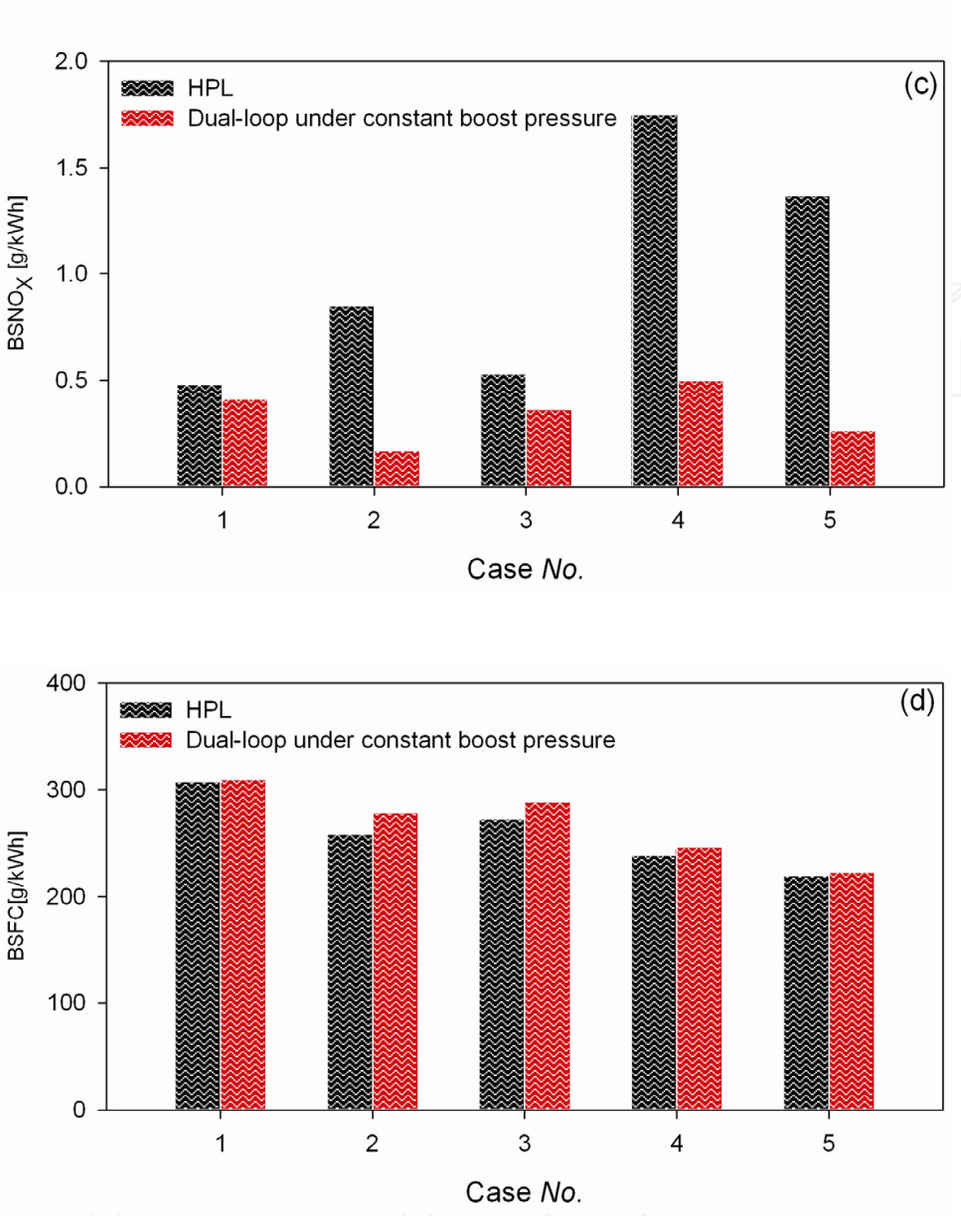

Figure 8. Simulation results comparison between HPL and dual-loop EGR under constant boost pressure; (a) Torque, (b) EGR rate, (c) BSNOx and (d) BSFC

3.2.2. Optimization of dual-loop EGR system

To compensate torque and BSFC under constant boost pressure condition, optimization was performed maintaining original boost pressure (bar). By advancing SOI and increasing injection mass, torque and BSFC could be compensated. Table 7 and 8 show results of optimization for constant torque and BSFC with controlled variables.

Figure 9 shows simulation results of HPL and Dual loop EGR under constant boost pressure and optimized Dual Loop EGR, respectively. 8% of torque and 5% of BSFC improvement were achieved on an average compared to the dual loop EGR system under constant boost pressure. Furthermore, higher NOx reduction efficiency appeared at each case except case 4.

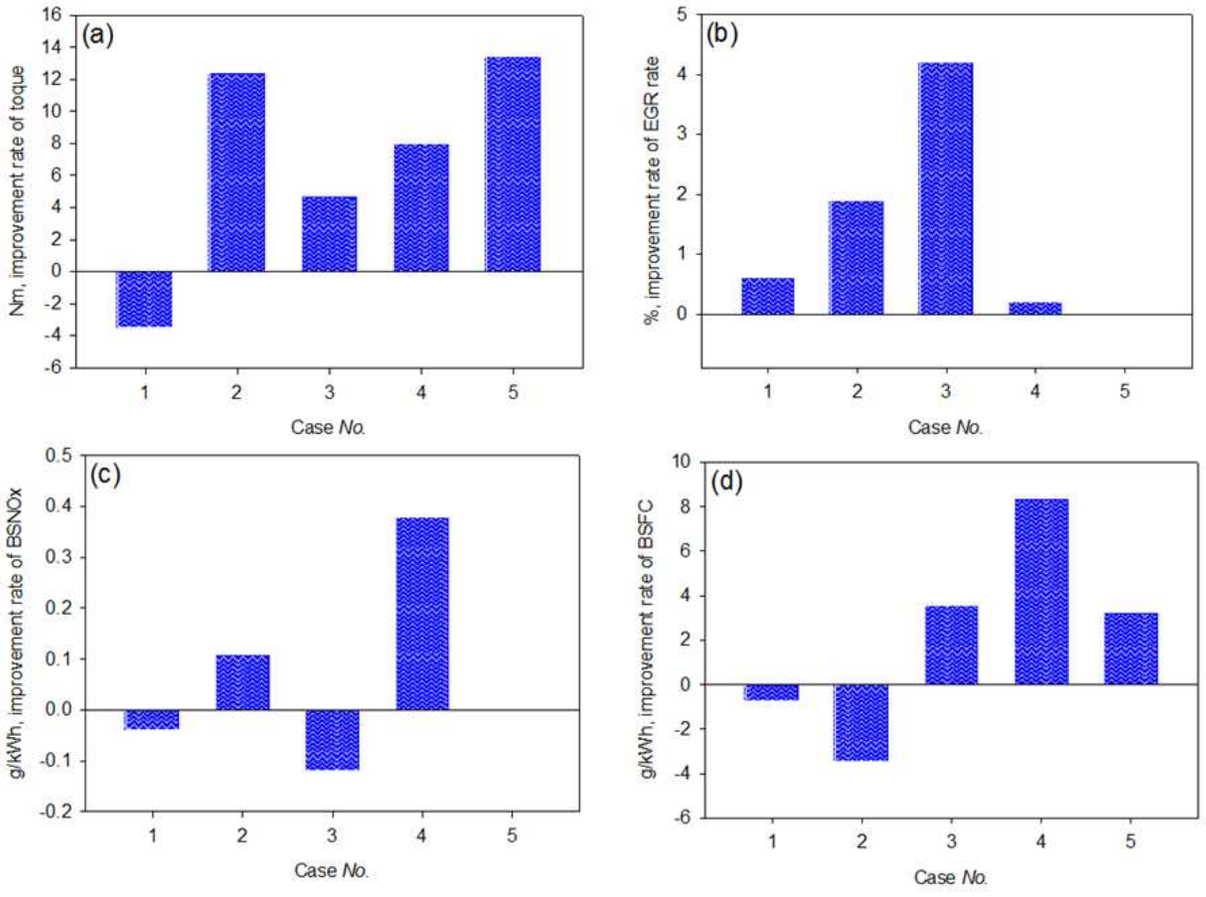

Figure 9. Results deviation of optimized dual-loop EGR compared to dual-loop EGR under constant boost pressure: (a) Torque, (b) EGR rate, (c) BSNOx and (d)BSFC

Controlled factors	Case1	Case 2	Case 3	Case 4	Case 5
HPL valve	12% open	3% open	23% open	12% open	7% open
LPL valve	12% open	9 % open	13.5% open	17% open	8% open
Injection mass	+1.5%	+3%	+2.9%	+2.5%	+1%
SOI	-	3 CA adv.	3 CA adv.	3CA adv.	1.2CA adv.
Flap valve	-	-	-	8% open	5% open
TC RPM	+2500	+2500	+5000	+1000	+2000

Table 7. Predicted values

Validation results					
Torque (N-m)	52.24	111.67	82.03	223.87	207.84
BSFC (g/kW-h)	307.2	255.27	276.25	247.01	233.30
EGR rate (%)	24.60	35.48	29.26	19.21	30.13
BSNOx (g/kW-h)	0.37	0.28	0.24	0.88	0.22

Table 8. Validation results

In case 4 (1556RPM / BMEP 9.93bar), it seemed that controlled variables which affect torque and BSFC were decoupled with the NOx reduction rate due to relatively high load conditions. It was necessary to control the variables sensitively at high load conditions.

For the optimized dual loop EGR system, 60% improvement of deNOx efficiency was achieved with increasing the EGR rates through all the cases when compared to results for the HPL system.

4. Conclusions

In this study, engine simulation was carried out to optimize the dual loop EGR system at 5 different engine operating conditions. As a result, the dual loop EGR system in a light-duty diesel engine had the potential to satisfy future emission regulations by controlling the dominant variables at given operating conditions. The details are as follows.

- An engine model for the HPL EGR was developed based on the experimental data at 5 operating conditions. The calibrated simulations showed within ±5% difference with the experimental results.
- Under constant boost pressure conditions, an average 60% NOx reduction was achieved in the dual loop EGR system compared to the results under the HPL system. However, approximately 8% of torque loss and 8% of BSFC loss occurred respectively.
- To compensate torque and fuel consumption, independent variables, such as start of injection and injection mass, were selected as additional control factors. Comparing these variables to the dual loop EGR system under constant boost pressure, approximately 8% of torque and 5% BSFC improvement were achieved except at high load conditions (case 4).

For the optimized dual loop EGR system, 60% improvement of deNOx efficiency was achieved with increasing EGR rate through all the cases compared to results for the HPL system.

Author details

Jungsoo Park
The Graduate School, Department of Mechanical Engineering, Yonsei University, Sinchon-dong, Seodaemun-gu, Seoul, Korea

Kyo Seung Lee
Department of Automotive Engineering, Gyonggi College of Science and Technology, Jeongwang-dong, Siheung-si, Gyonggi-do, Korea

5. References

Johnson, T. V. (2011), Diesel Emissions in Review, *SAE International Journal of Engines* 2011-01-0304, Vol. 4, No. 1. 143-157, doi:10.4271/2011-01-0304.

Zheng, M.; Reader, G. T. & Hawley, J. G. (2004), Diesel Engine Exhaust Gas Recirculation – A Review on Advanced and Novel Concepts, *Energy Conversion & Management*, Vol. 45, No.6, (April 2004), pp. 883-900, ISSN 0196-8904

Yamashita, A.; Ohki, H., Tomoda, T. & Nakatami, K. (2011), Development of Low Pressure Loop EGR System for Diesel Engines, *SAE Technical Paper* 2011-01-1413, ISSN 0148-7191, Detroit, Michigan, USA, April , 12-14, 2011

Cho, K.; Han, M., Wagner, R. M. & Sluder, C. S. (2008), Mixed-source EGR for Enabling High Efficiency Clean Combustion Mode in a Light-duty Diesel Engine, *SAE International Journal of Engines*, Vol. 1, No. 1, 99. 457-465, ISSN 1946-3944

Adachi, T.; Aoyagi, Y., Kobayashi, M., Murayama, T., Goto Y. & Suzuki H. (2009), Effective NOx Reduction in High Boost, Wide Range and High EGR Rate in a Heavy Duty Diesel Engine, *SAE Technical Paper* 2009-01-1438, ISSN 0148-7191, Detroit, Michigan, USA, April , 20-23, 2009

Kobayashi, M.; Aoyagi, Y., Adachi, T., Murayama, T., Hashimoto, M., Goto, Y. & Suzuki, H. (2011), Effective BSFC and NOx Reduction on Super Clean Diesel of Heavy Duty Diesel Engine by High Boosting and High EGR Rate, *SAE Technical Paper* 2011-01-0369, ISSN 0148-7191, Detroit, Michigan, USA, April , 12-14, 2011

Wang, J. (2008), Air Fraction for Multiple Combution Mode Diesel Engines with Dual-loop EGR System, *Control Engineering Practice*, Vol. 16, No. 12, (December 2008), pp. 1479-1486, ISSN 0967-0661

Yan, F. & Wang, J.(2010), In-cylinder Oxygen Mass Fraction Cycle-by-Cycle Estimation via a Lyapunov-based Observer Design, *IEEE 2010 American Control Conference*, pp. 652-657, ISBN 978-1-4244-7426-4, Baltimore, Maryland, USA, June 30- July 02, 2010

Yan, F. & Wang, J.(2011), Control of Dual Loop EGR Air-Path Systems for Advanced Combustion Diesel Engines by a Singular Perturbation Methodology, *IEEE 2011 American Control Conference*, pp. 1561-1566, ISBN 978-1-4577-0080-4, San Francisco, California, USA, June 29- July 01, 2011

Mueller, V.; Christmann, R., Muenz, S. & Gheorghiu, V. (2005), System Structure and Controller Concept for an Advanced Turbocharger/EGR System for a Turbocharged Passenger Car Diesel Engine, *SAE Paper No.* 2005013888.

Shutty, J. (2009), Control Strategy Optimization for Hybrid EGR Engines, *SAE Technical Paper* 2009-01-1451, ISSN 0148-7191, Detroit, Michigan, USA, April , 20-23, 2009

Lee, S. J.; Lee, K. S., Song, S. & Chun, K. M. (2006), Low Pressure Loop EGR System Analysis Using Simulation and Experimental Investigation in Heavy-duty Diesel Engine, *International Journal of Automotive Technology,* Vol.7, No. 6, (October 2006), pp. 659-666, ISSN 1229-9138

Park, J.; Lee, K. S., Song, S. & Chun, K. M. (2010), A Numerical Study for Light-duty Diesel Engine with Dual Loop EGR System under Frequent Engine Operating Conditions by Using DOE, *International Journal of Automotive Technology,* Vol.11, No. 5, (October 2010), pp. 617-623, ISSN 1229-9138

Hiroyasu, H.; Kadota, T. & Arai, M. (1983), Development and Use of a Spray Combustion Modeling to Predict Diesel Engine Efficiency and Pollutant Emissions: Part 1

Combustion Modeling, *Bulletin of the JSME*, Vol. 26, No. 214, (April 1983), pp.569-575, ISSN 0021-3764

IntechOpen